

MINERALOGICAL MAGAZINE

VOLUME 40 NUMBER 310 JUNE 1975

Tacharanite

G. CLIFF,¹ J. A. GARD,² G. W. LORIMER,¹ AND H. F. W. TAYLOR²

SUMMARY. Tacharanite has been re-examined using electron microscopy and diffraction, analytical microscopy, X-ray powder and fibre rotation photographs, and other methods. The composition approximates to $\text{Ca}_{12}\text{Al}_2\text{Si}_{18}\text{O}_{68}\text{H}_{36}$, and the X-ray diffraction patterns can be referred to an *A*-centred monoclinic pseudo-cell with *a* 17.07, *b* 3.65, *c* 27.9 Å, β 114.1°, *Z* = 1. In the true cell *b* is certainly, and *a* and *c* probably, doubled. Small, reversible changes in pseudo-cell parameters occur on heating below 200 °C, and parameters found by electron diffraction differ slightly from those found with X-rays, presumably due to shrinkage on dehydration in the high vacuum of the electron microscope. An earlier report that tacharanite changes into a mixture of tobermorite and gyrolite on standing in air is not confirmed. Tacharanite shows some important resemblances to tobermorite, but there are also significant differences.

SWEET (1961) described a new mineral from Portree, Scotland, which she named tacharanite. It was a calcium silicate hydrate, with appreciable amounts of Al and other elements; the chemical analysis, X-ray powder pattern, thermal weight loss curve, specific gravity, and mean refractive index were given. The composition and powder pattern suggested a resemblance to tobermorite. Tacharanite has since been reported from Mull, Scotland (Walker, 1971), Carneal, N. Ireland (Sabine and Young, 1972), Bramburg, Germany (Koritnig, 1972), and Huntly, Scotland (Livingstone, 1974). Through the kindness of Miss Sweet, Dr. Sabine, Professor Koritnig, and Dr. Livingstone, we have examined small portions of these specimens.

General description, optical properties, and specific gravity

Sweet (1961) described the Portree material as cryptocrystalline, with mean refractive index slightly below 1.537 and D_4^{23} 2.36, though the densities of individual fragments varied. Sabine and Young (1975) described the Carneal material as isotropic, with refractive index partly 1.530, but mainly 1.500–1.510, perhaps due to lower crystallinity. Koritnig (1972) described the Bramburg mineral as forming spherulites or bundles of fibres with \pm elongation, usually in a matrix of isotropic material, possibly calcium silicate hydrate gel. We find the bulk material of this specimen to have a mean index of 1.54 and a specific gravity of 2.33, determined by suspension. We find the Huntly material to consist of fibre aggregates; X-ray photographs

¹ Department of Metallurgy, The University, Manchester, England.

² Department of Chemistry, University of Aberdeen, Scotland.

show that these are composed of crystallites aligned with their *b*-axes nearly parallel to the fibre direction, but with almost completely random orientation in the sense of rotation around this direction. The refractive indices, using white light, are 1.530 for light vibrating parallel to the fibres and 1.518 for light vibrating perpendicularly to them. The specific gravity is 2.36. The variability in properties of different specimens suggests that tacharanite often occurs in a matrix of less crystalline material, which is possibly similar to the gelatinous plombierite described by McConnell (1954). The crystallinity is possibly highest in the specimens from Portree and Huntly, and lowest in that from Carneal.

Sweet (1961) reported that, on standing in air, tacharanite changes spontaneously into a mixture of tobermorite and gyrolite. We do not confirm this for any of the specimens that we have examined, and Sabine and Young (1975) state that a specimen of the Carneal mineral that had been kept in a dry, heated building for 9½ years gave the X-ray powder pattern characteristic of tacharanite (I.G.S. NI 1591).

Electron microscopy and diffraction

Samples of tacharanite from Bramburg, Carneal, and Huntly were examined with an AEI type EM802 electron microscope equipped with a 60° double-tilt specimen

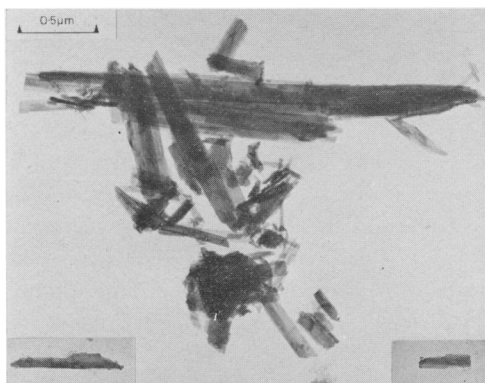


FIG. 1. Electron micrograph of tacharanite from Bramburg, Germany. Crystals used for electron diffraction are shown in the lower corners.

cartridge (Lucas, 1970). In each case, a small sample of material was crushed in isopropyl alcohol on a glass slide, and a specimen grid carrying a carbon film was momentarily brought in contact with the liquid surface. Some specimens were coated with aluminium evaporated in vacuum as an internal standard for electron diffraction. An electron micrograph (fig. 1) of the Bramburg mineral shows that it occurs as aggregates of very thin laths up to several micrometres long. Isolated crystals suitable for electron diffraction were difficult to find and were very small. The Bramburg specimens were almost pure tacharanite, but the

Carneal specimen contained a large proportion of material that gave no diffraction patterns and that resembled plombierite (McConnell, 1954); the Huntly specimens were mostly fibre bundles associated with well-crystallized fragments that were identified by electron diffraction as scawtite (see Livingstone, 1974). Most of the electron-diffraction data were obtained from the Bramburg specimens, but identical sets of patterns were given by the laths in specimens from all three localities.

Several series of electron-diffraction patterns were first recorded from laths tilted around their long *b**-axes. All these patterns, which represent *h*0*l* zones, contained sharp spots and streaks. The spots fell on rectangular nets, with layer rows indicating

a b -period of 3.64 Å. Spots in the odd-layer rows, where present, were normally centred with respect to those in even-layer rows. The layer rows of spots were interspaced with weak streaky reflections showing that b is doubled in the true unit cell. Many crystals gave the pattern shown in fig. 2*a* at a small angle of tilt, suggesting that this zone is close to the principal cleavage plane. From this orientation, 22° tilt round b^* gave the pattern shown in fig. 2*c*, which has a row of spots spaced $(15.56 \text{ Å})^{-1}$ apart. This row was called a^* , as it had the closest spacing observed in any zone. The 100, 300, 500, 700, and 10.0.0 spots were more intense than the other $h00$ spots. 45° tilt in the opposite direction gave a pattern with a row spaced $(12.4 \text{ Å})^{-1}$ (see fig. 2*b*), at first erroneously thought to be c^* . Numerous other hol zones were recorded, but difficulties in measuring angles of tilt were encountered because most particles comprised more than one crystal in slightly different orientations. A projection down b^* of the reciprocal lattice was constructed, and, after some adjustments, this could be indexed as an A -centred monoclinic pseudo-cell, with β^* approximately 67°. The recorded 12.4 Å reflection was indexed $\bar{1}02$.

In order to refine β^* , several series of zones were recorded by tilting crystals around their a^* -axes, so that the $[0\bar{1}1]$, $[0\bar{3}1]$, $[0\bar{5}1]$, and $[0\bar{7}1]$ zone axes were in turn placed parallel to the electron beam. Examples of the first three zones are shown in figs. 2*d*, *e*, and *f*, respectively. The corresponding $[011]$, $[031]$, etc., zones were also recorded by tilting in the opposite direction. Each pair of diffraction patterns appeared to be identical mirror images. Comparisons of d spacings for numerous hkl and corresponding $h\bar{k}l$ reflections measured on these patterns suggested that γ^* might deviate from 90° by as much as 0.5°, but the differences varied from one crystal to another, and the pseudo-cell was provisionally assumed to be monoclinic within the accuracy of measurement. Each diffraction pattern was then placed in turn on a Pye two-way measuring microscope with a^* exactly parallel to the x -direction of traverse. The reciprocal distances, e.g. y_5 and Δx_5 , shown in fig. 2*f* for the $[0\bar{5}1]$ zone, were measured and converted to Å⁻¹ units, using a procedure described elsewhere (Gard, 1971). These values were then used to calculate c and β^* as follows: $c = 5(y_5^2 - y_0^2)^{-\frac{1}{2}}$; $\cot \beta^* = 2(c \cdot \overline{\Delta x_2})^{-1}$, where $\overline{\Delta x_2}$ is the average value of $(\Delta x_5 - \Delta x_3)$, $(\Delta x_3 - \Delta x_1)$, $(\Delta x_1 + \Delta x_7)$ etc.; the slight systematic distortion due to astigmatism of the imaging lenses of the electron microscope is compensated by use of $\overline{\Delta x_2}$ rather than Δx_5 , Δx_3 etc. The values of c and β^* were used to construct the $[100]$ and $[010]$ projections of the reciprocal lattice shown in fig. 3. The pseudo-cell that best fitted the data had a 16.85, b 3.64, c 27.36 Å, β 112.1°.

Several series of diffraction patterns were next recorded by rotating crystals around the 12.4 Å row of spots. All these patterns could be indexed as $[2V1]$ zones with values of V up to seven, confirming the $\bar{1}02$ indices for the 12.4 Å reflection. One of these patterns, the $[211]$ zone, is shown in fig. 2*b*. All attempts to record the $[100]$ zone were unsuccessful because of the excellent (001) cleavage of the crystals. Certain reflections were notably intense on all diffraction patterns in which they appeared. They were $\bar{1}02$ (12.4 Å), $\bar{3}15$ (2.85 Å), $\bar{3}13$ (3.025 Å), $\bar{3}11$ (3.039 Å), and 020 (1.82 Å); these probably correspond to the strong lines at 12.7, 3.048, 2.89, and 1.822 Å that are present in the X-ray powder photographs (Table I).

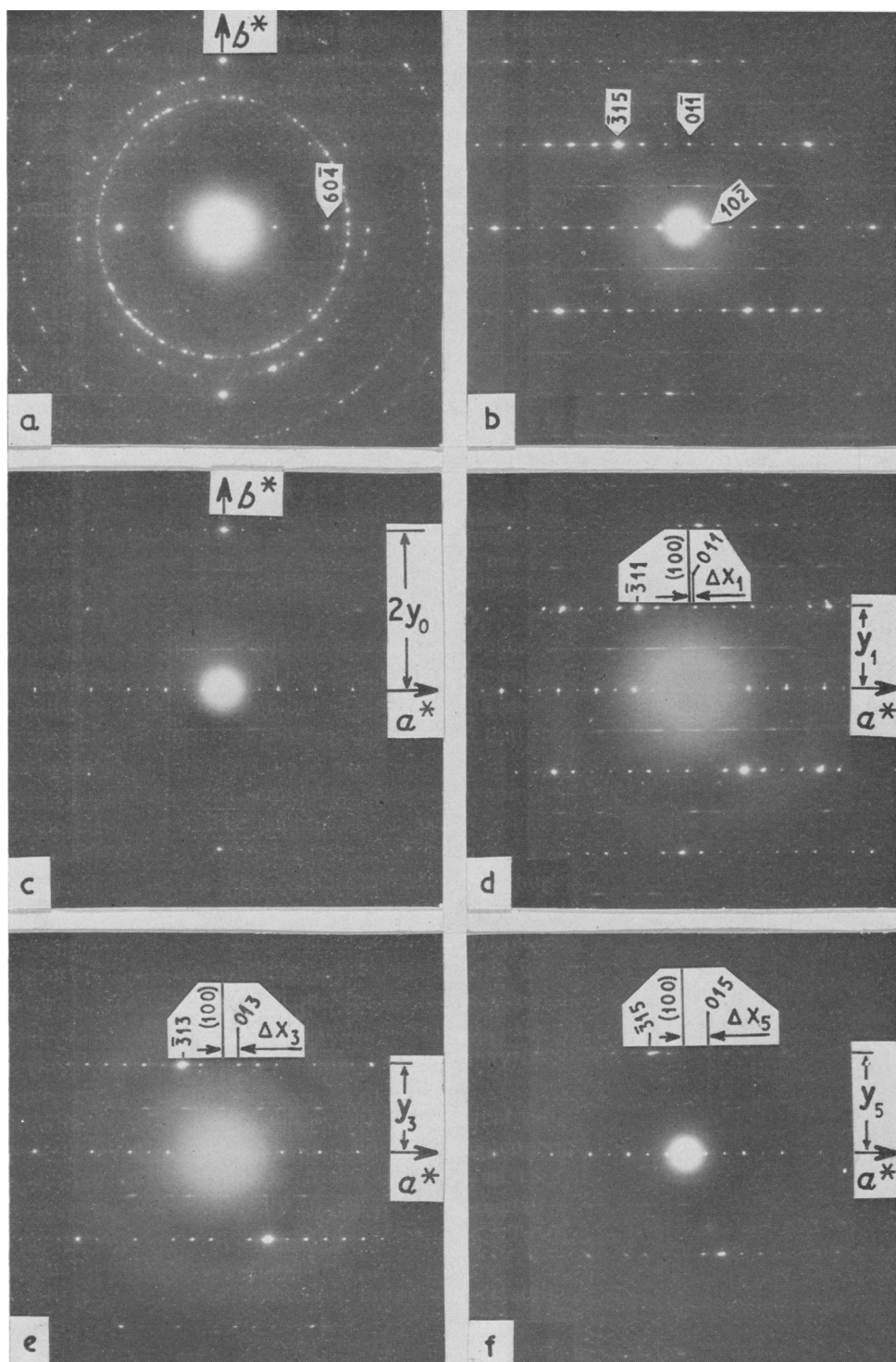


FIG. 2.

Attention was next directed to the weak streaky reflections that define the true unit cell. As for other fibrous calcium silicates, b is definitely doubled, but otherwise there is considerable disorder. The streaks are stronger in the $[011]$ zone than in the $[001]$ zone (fig. 2*d* and *c*, respectively), and they are less diffuse in the $[2V1]$ zones (e.g. fig. 2*b*) than in the $[0V1]$ zones, suggesting that c is doubled, and that streaking is

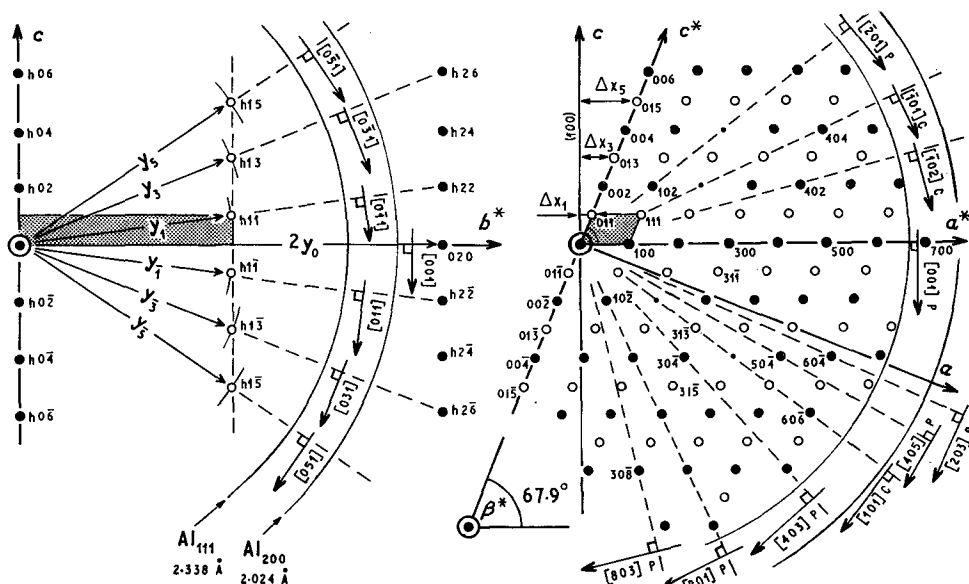


FIG. 3. $[100]$ and $[010]$ projections of the reciprocal lattice of vacuum-dehydrated tacharanite, indexed on the pseudo-cell, which is shaded. The zone axes of recorded electron-diffraction patterns, and the co-ordinates y_V and Δx_V measured on the patterns, are indicated. Full circles represent reciprocal lattice points in planes with k even, and open circles, points with k odd. P after the zone-axis symbol indicates that the corresponding diffraction pattern is primitive, with no spots having k odd; C indicates that it is centred and contains spots with both odd and even values of k .

more pronounced parallel to a^* than parallel to c^* . Consideration of maxima on the streaks in all diffraction patterns indicated that both a and c are doubled in the true cell. The true cell is therefore probably F -centred monoclinic (an unconventional cell that retains the pseudo-cell axes), with a , b , and c double those of the pseudo-cell.

X-ray powder and fibre rotation patterns

Table I, col. 2 gives the observed powder pattern for the Bramburg specimen, obtained using a diffractometer and a Guinier camera, both with copper radiation.

FIG. 2. Electron-diffraction patterns from single crystals of tacharanite from Bramburg, Germany. (a) The crystal has $[203]$ parallel to the electron beam, i.e. the (001) cleavage plane almost normal to the beam. The rings are from aluminium used as an internal standard. (b) $[211]$ parallel to the beam. (c) to (f) were recorded from a crystal rotated round a^* to bring the $[001]$, $[011]$, $[031]$, and $[051]$ zone axes, respectively, parallel to the beam. The co-ordinates marked y_V and Δx_V were measured with a Pye two-way measuring microscope.

TABLE I. *X-ray powder and fibre rotation data for tacharanite (Cu-K α radiation)*

1 Calculated		2 Observed		3 Observed	4 Observed		5 Observed	
<i>hkl</i>	<i>d</i>	<i>d</i>	<i>I</i> _{rel}	<i>k</i> _{true}	<i>d</i>	<i>I</i> _{rel}	<i>d</i>	<i>I</i> _{rel}
100	15.58 Å	—	—	—	—	—	—	—
002, $\bar{1}02$	12.73	12.7	vvs	0	12.7	vvs	12.7	vvs
102, $\bar{2}02$	8.33	8.34	mw	0	8.40	m	8.36	w
200	7.79	—	—	—	—	—	—	—
104	6.98	7.1	vw ⁶	1	7.10	vw ⁶	7.05	vw ⁶
004, $\bar{2}04$	6.37	6.4	vwv	—	6.31	vwv	—	—
202, $\bar{3}02$	5.69	5.69	mw	0	5.66	mw	5.65	mw
104, $\bar{3}04$	5.20	—	—	—	—	—	—	—
300	5.19	5.19	ms	0	5.16	ms	{ 5.25 5.10	{ w m
$\bar{1}06$, $\bar{2}06$	4.60	—	—	—	—	—	—	—
006, $\bar{3}06$	4.24	—	—	—	—	—	—	—
302, $\bar{4}02$	4.24	—	—	—	—	—	—	—
204, $\bar{4}04$	4.166	4.145	vwv	—	4.16	vwv	—	—
400	3.896	—	—	—	—	—	—	—
106, $\bar{4}06$	3.727	3.736	w	0	3.75	w	—	—
011	3.613	—	—	—	—	—	—	—
$\bar{1}11$	3.565	—	—	—	—	—	—	—
$\bar{2}08$	3.488	3.489	w	0	3.49	vw	—	—
111	3.476	—	—	—	—	—	—	—
$\bar{1}08$, $\bar{3}08$	3.403	3.405	m	0	3.37	m	—	—
304, $\bar{5}04$	3.401							
$\bar{1}13$	3.393	—	—	—				
402, $\bar{5}02$	3.361	—	—	—				
013	3.353	—	—	—				
$\bar{2}11$	3.353	3.353	w	2				
$\bar{2}13$	3.278	3.273	vwv	—	—	—	—	—
206, $\bar{5}06$	3.216	—	—	—	—	—	—	—
211	3.208	3.206	vwv	—	—	—	—	—
008, $\bar{4}08$	3.183	3.178	w	2, 0	3.16	vwv	—	—
113	3.175							
500	3.116	—	—	—	—	—	—	—
$\bar{1}15$	3.051	—	—	—	—	—	—	—
$\bar{3}13$	3.050	3.048	vs	2	3.05	vs	3.043	vs
$\bar{3}11$	3.050							
$\bar{2}15$	3.022	—	—	—	—	—	—	—
015	2.967	2.980	vwv	—	2.98	vwv	—	—
213	2.914	—	—	—	—	—	—	—
108, $\bar{5}08$	2.896	—	—	—	—	—	—	—
$\bar{3}15$	2.889	2.888	ms	2	2.89	s	2.86	ms/b
311	2.889							
404, $\bar{6}04$	2.846	2.853	ms	0	—	—	—	—

1. Calculated for a monoclinic pseudo-cell with a 17.07, b 3.65, c 27.9 Å, β 114.1°. All spacings are listed that have $d > 2.2$ Å; for lower d -spacings, only those corresponding to observed reflections are listed.

2. Observed powder data for Bramburg specimen.

3. Observed k indices from fibre rotation pattern for the Huntly specimen, referred to the true cell with $b = 7.3$ Å.

4. Observed powder data for Portree specimen (Sweet, 1961).

5. Observed powder data for the Bramburg specimen at 200 °C.

6. The observed spacing of 7.05–7.1 Å is not 104, but has $k = 1$ referred to the true cell.

TABLE I. (cont.)

1 Calculated		2 Observed		3 Observed	4 Observed		5 Observed	
<i>hkl</i>	<i>d</i>	<i>d</i>	<i>I_{rel}</i>	<i>k_{true}</i>	<i>d</i>	<i>I_{rel}</i>	<i>d</i>	<i>I_{rel}</i>
115	2·795	—	—	—	—	—	—	—
2·0.10, 3̄·0.10	2·779	—	—	—	—	—	—	—
306, 606	2·777	2·775	s	0	2·79	s	2·745	ms/b
502, 602	2·776							
413	2·772							
411	2·729	2·731	vvw	2	—	—	—	—
1̄·0.10, 4̄·0.10	2·694	—	—	—	—	—	—	—
217	2·689	—	—	—	—	—	—	—
415	2·688	2·687	vvw	2	2·69	vvw	—	—
117	2·670	—	—	—	—	—	—	—
317	2·631	—	—	—	—	—	—	—
313	2·630	—	—	—	—	—	—	—
208, 6̄08	2·598	—	—	—	—	—	—	—
600	2·597	—	—	—	—	—	—	—
017	2·577	2·581	vvw	2	2·59	vvw	—	—
215	2·576	—	—	—	—	—	—	—
411	2·576	—	—	—	—	—	—	—
0·0.10, 5̄·0.10	2·546	—	—	—	—	—	—	—
417	2·509	2·509	vw	2	2·495	vw	—	—
513	2·492	2·491	vw	2				
515	2·461	—	—	—	—	—	—	—
504, 7̄04	2·434	2·434	ms	0, 2	2·440	m	2·417	mw
117	2·432							
511	2·431	—	—	—	—	—	—	—
406, 7̄06	2·419	—	—	—	—	—	—	—
1·0.10, 6̄·0.10	2·364	2·367	vw	0	2·375	vvw	—	—
602, 7̄02	2·363	—	—	—	—	—	—	—
219	2·361	—	—	—	—	—	—	—
413	2·360	—	—	—	—	—	—	—
319	2·347	—	—	—	—	—	—	—
315	2·347	—	—	—	—	—	—	—
517	2·347	—	—	—	—	—	—	—
3̄·0.12	2·325	—	—	—	—	—	—	—
308, 7̄08	2·324	—	—	—	—	—	—	—
119	2·322	—	—	—	—	—	—	—
2̄·0.12, 4̄·0.12	2·300	2·295	vvw	0	2·295	vvw	—	—
511	2·295							
419	2·284	—	—	—	—	—	—	—
217	2·259	—	—	—	—	—	—	—
019	2·236	2·234	vvw	—	—	—	—	—
615	2·235							
613	2·235							
2·0.10, 7̄·0.10	2·173	2·176	vw	0	2·185	vw	—	—
415	2·129	2·128	mw	2	2·130	mw	—	—
317	2·081	2·077	vw	2	2·080	vw/b	—	—
2̄·1.11	2·073							
702, 8̄02	2·055	2·053	vvw/d	0	—	—	—	—
4̄·1.11	2·054							
619	2·054							
611	2·053							

TABLE I. (cont.)

1 Calculated		2 Observed		3 Observed	4 Observed		5 Observed	
<i>hkl</i>	<i>d</i>	<i>d</i>	<i>I</i> _{rel}	<i>k</i> _{true}	<i>d</i>	<i>I</i> _{rel}	<i>d</i>	<i>I</i> _{rel}
1.0.12, $\bar{7}$.0.12	1.996	1.993	mw	2	2.005	m	—	—
$\bar{3}$.1.11	1.994							
$\bar{7}$ 1.7	1.994							
800	1.948	1.948	mw	2	1.952	mw	—	—
$\bar{7}$ 11	1.946							
$\bar{7}$ 19	1.917							
$\bar{6}$.1.11	1.910	1.913	vw	2	1.915	vw	—	—
417	1.910							
508, $\bar{5}$ 08	1.876	1.873	vww	—	—	—	—	—
704, $\bar{5}$ 04	1.876							
$\bar{3}$.1.13	1.849	1.851	w	2	1.850	mw	—	—
319	1.849							
711	1.848							
020	1.825	1.822	s	4	1.820	ms	1.825	s
022	1.807	1.805	w	—	—	—	—	—
$\bar{1}$ 22	1.807							
222, $\bar{3}$ 22	1.738	1.735	mw	0	1.738	mw	—	—
3.0.12, $\bar{9}$.0.12	1.732							
$\bar{9}$ 17	1.679	1.676	mw	2	1.675	m	—	—
$\bar{9}$ 15	1.679							
$\bar{9}$ 19	1.651	1.649	m	2	1.641	m	—	—
$\bar{9}$ 13	1.651							
2.0.14, $\bar{9}$.0.14	1.630	1.633	vww	—	—	—	—	—
$\bar{2}$ 28	1.617	1.613	vww	2	—	—	—	—
$\bar{8}$.1.13	1.611							
617	1.611							
10.0.0	1.558	1.563	vww	—	—	—	—	—
$\bar{6}$ 24	1.536	1.537	mw	4	1.536	ms/b	—	—
$\bar{6}$ 26, $\bar{6}$ 22	1.525	1.526	mw	4				
		1.490	vww					
		1.460	vw					
		1.431	vw					
		1.414	vw					
		1.386	vw					
		1.363	vw					
		1.316	vww					
		1.296	vww					
		1.248	vww					
		1.220	w					
		1.198	vw					
		1.118	w					
		1.110	vww					
		1.074	vww					
		1.068	vw					

Corundum (trigonal, a 4.758, c 12.991 Å; Swanson and Fuyat, 1953) was used as an internal standard for spacings. The Guinier films had somewhat heavy backgrounds, supporting the view that poorly crystalline material was present. The Portree and Huntly specimens gave closely similar results, and the pattern agrees well with that reported by Sweet (1961) for the Portree material (col. 4). The Portree specimen also gave a weak line at 11.3 Å, probably due to tobermorite.

A fibre rotation pattern was obtained for the Huntly specimen; the layer line spacing was found to be about 7.3 Å, in agreement with the value of b found by electron diffraction. There was very strong pseudo-halving of b , the only indication that the true value was 7.3 and not 3.65 Å being a streak running along the first true layer, from $\xi = 0$ to about 0.07 Å⁻¹. Table I, col. 3, gives the k -indices of reflections observed on the fibre rotation pattern, referred to the true b -axis of 7.3 Å.

Except for the streak mentioned above, it is most unlikely that any of the reflections with odd k -indices are strong enough to contribute to the powder pattern. The latter cannot be indexed satisfactorily using the pseudo-cell parameters found by electron diffraction, but it can be indexed if slightly different parameters are assumed, viz. A -centred monoclinic with a 17.07, b 3.65, c 27.9 Å, β 114.1° ($V = 1586.8$ Å³). This cell is equivalent to a face centred, geometrically orthorhombic one of four times the volume, with a 62.33, b 3.64, c 27.9 Å. Spacings calculated for the monoclinic cell (Table I, col. 1) agree satisfactorily with those observed (col. 2), and there appeared to be reasonable agreement between intensities on the powder pattern and those on the electron-diffraction patterns. The k -indices corresponding to the calculated spacings agree with those observed on the fibre rotation pattern. The pseudo-cell for X-ray diffraction differs from that found with electron diffraction mainly in the values of a and β , differences in other parameters being probably not significant.

X-ray powder studies of heated or evacuated material

A specimen of the Portree material, weighing under 1 mg, was heated successively to 100°, 260°, 400°, and 580 °C, each for 4 to 5 hr, and to 700°, 800°, and 1000 °C, each for 2 hr; after each heating the specimen was cooled to room temperature and a powder pattern obtained, using a 6-cm-diameter camera. The products cooled from 100 to 580 °C gave virtually unaltered patterns of tacharanite. Those cooled from 700 to 800 °C gave weakened tacharanite patterns, with an intensified line at 3.49 Å, while that cooled from 1000 °C gave a pattern of wollastonite. A sample of the Bramburg specimen that had been heated at 500 °C for 5 hr gave a pattern virtually identical with that of the original material.

Dr. A. R. West kindly made for us some high-temperature Guinier powder patterns, using the Bramburg specimen and a Nonius-Lenne camera of 11.46 cm diameter. If the sample was heated in air at about 5 deg hr⁻¹, small changes in the pattern, indicative of changes in lattice parameters, occurred at 50–150 °C. The shifts in spacings were continuous, and no significant further changes occurred below 700 °C. Table I, col. 5, gives the 200 °C pattern; the paucity of lines is probably due to limitations in the technique and not to reduction in crystallinity. If a sample was heated in air to 150–500 °C and then cooled, also at about 5 deg hr⁻¹, the changes in pattern were

reversed at 100–50 °C. Reversion of the pattern did not occur if cooling was in dry N₂, but it occurred within a few hours if the sample was subsequently allowed to stand in air at room temperature. A sample was cycled several times in air between room temperature and 200–500 °C; the changes in pattern appeared to be reversible repeatedly. When the sample temperature reached 700–800 °C, wollastonite was formed. Some extra lines appeared at about 850 °C, at 6.44, 3.72, 3.22, and 2.64 Å; the 3.22 Å line disappeared again at about 900 °C, but the others remained until 940 °C, the highest temperature used.

Samples of the Bramburg and Huntly materials were also examined in a vacuum, using a Guinier camera. The pressure was held at 0.01 torr for 2 hr before the start of the exposure and during it. This pressure is not as low as that existing in the electron microscope ($< 10^{-4}$ torr). The pattern showed barely detectable changes, much smaller than those observed at 150 °C or above.

The fact that the change in lattice parameters observed on heating is reversed on cooling in air, but not in dry N₂, suggests that the effect is associated with a reversible loss of water. The observations possibly explain the difference between the pseudo-cell parameters found with X-rays and those found with electron diffraction; dehydration could have occurred in the electron microscope. *d*-spacings calculated using the cell found with electron diffraction gave mediocre agreement with those observed at 200 °C, but the test is unsatisfactory because the monoclinic pseudo-cell found by electron diffraction, unlike that found with X-rays, is not equivalent to a larger one that is geometrically orthorhombic. This increases the number of calculated spacings, so that small adjustments in parameters would make it possible to obtain a better match with the observed spacings, which would, however, be of doubtful significance.

No explanation is offered for the powder spacings appearing at 850–940 °C that were not due to wollastonite.

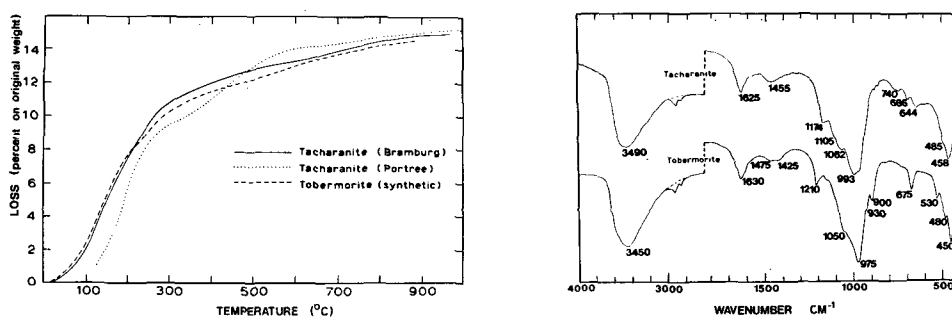
Thermogravimetry and infrared absorption

Fig. 4 gives a t.g. curve for the Bramburg specimen, obtained in air at 15 °C min⁻¹ on a 15 mg sample, using a Dupont 950 instrument. For comparison, curves are included for a typical synthetic tobermorite, obtained under the same conditions, and for the Portree tacharanite (Sweet, 1961). Sweet did not state the heating conditions that she used; the differences between her results and those for the Bramburg specimen below about 500 °C could be explained if she had used a slower heating rate or static heating conditions. The curve for the Bramburg specimen closely resembles that for the tobermorite.

Fig. 5 gives the infrared absorption spectrum of the Bramburg specimen, with one of a typical tobermorite for comparison. The resemblances between the two spectra are closer than those between either of them and the spectra of other calcium silicate minerals such as xonotlite. In addition to the Si–O bands, both spectra indicate the presence of molecular water, with or without additional hydroxyl, and of small amounts of CO₃²⁻, which could be present within the silicate structures. The tacharanite specimen was also examined after being heated at 500 °C; the bands due to water were weakened, but in other respects the spectrum was almost unchanged.

Analytical electron microscopy

Chemical analyses of the Bramburg and Huntly specimens were carried out in the analytical electron microscope EMMA-4 operating at an accelerating voltage of 100 kV. The X-rays were detected and analysed with an energy-dispersive detector coupled to the necessary ancillary electronics. The characteristic X-ray intensities of the Al-K, Si-K, K-K α , and Ca-K α lines were recorded simultaneously using the energy dispersive system and the integrated counts were determined for each of the characteristic X-ray peaks in question with the background counts subtracted. An individual analysis took approximately 300 seconds.



FIGS. 4 and 5: FIG. 4 (left). Thermogravimetric curves for tacharanite from Bramburg and for a synthetic tobermorite, obtained in air at 15 °C min⁻¹, and (Sweet, 1961) for tacharanite from Portree (heating conditions not given). FIG. 5 (right). Infrared absorption spectra for tacharanite (Bramburg) and for a tobermorite from Portree, Scotland. The KBr disc method was used and the doublet absorptions near 2900 cm⁻¹ are caused by organic impurities.

Previous work with the analytical electron microscope (Cliff and Lorimer, 1972; Lorimer, Nasir, Nicholson, Nuttall, Ward, and Webb, 1972; Lorimer and Champness, 1973) has shown that if the specimen is thin enough to carry out conventional transmission electron microscopy at 100 kV then it is transparent to the primary X-rays produced by the electron beam and corrections for X-ray absorption, and X-ray fluorescence can be neglected. Thus while the absolute intensity of the characteristic X-rays for any specific element will be a function of specimen thickness, the characteristic X-ray intensity ratio for any two elements will be independent of thickness, i.e. $C_1/C_2 = k \cdot I_1/I_2$, where C_1 and C_2 are the weight fractions of two elements, I_1 and I_2 are the observed intensities and k is a constant, which must be experimentally determined from the sample itself or thin standards.

During the present analysis a crushed sample of synthetic pseudo-wollastonite was used to obtain a k value for the Ca:Si ratio, an ion-thinned anorthite glass standard was used to determine k for the Al:Si ratio, and the k value for the K:Si ratio was assumed to be the same as that for Ca:Si. The results were then normalized to give 100% total oxides, excluding water, for each sample. No attempt was made to determine either water contents or absolute contents of the other constituents by this method.

Analytical results and atomic pseudo-cell contents

For the Bramburg specimen, it was assumed that the total weight loss found by thermogravimetry (fig. 4) was of water, and the results were recalculated to a total of 100 % including this constituent (Table II, col. 2). Not enough of the Huntly specimen was available for a t.g. curve to be determined; seven separate fibre bundles from this specimen were analysed, and col. 3 gives the mean results recalculated assuming the water content to be the same as for the Bramburg specimen. Col. 4 gives the standard errors on these mean results.

TABLE II. *Chemical analyses and atomic pseudo-cell contents for tacharanite*

	1	2	3	4		5	6
SiO ₂	41·8	48·3	48·5	0·3	Si	17·9	18·2
Al ₂ O ₃	5·6	4·5	5·5	0·1	Al	2·0	2·4
Fe ₂ O ₃	0·3	nil	nil	—	Fe	—	—
MgO	3·2	0·4	nil	—	Mg	0·2	—
CaO	33·6	30·8	30·0	0·2	Ca	12·2	12·1
Na ₂ O	0·6	0·5	nil	—	Na	0·4	—
K ₂ O	0·1	0·6	1·0	0·1	K	0·3	0·5
H ₂ O	15·2	14·9	14·9	—	H	36·8	37·3
Total	100·4	100·0	99·9		O	69·9	71·0

1. Analysis for tacharanite, Portree, B.M. 1961, 163, Sweet (1961); analyst D. I. Bothwell. Figure for H₂O includes a little CO₂.
2. Analysis for tacharanite, Bramburg, this investigation.
3. Analysis for tacharanite, Huntly, this investigation.
4. Standard errors on mean values in col. 3.
5. Atomic pseudo-cell contents for Bramburg specimen.
6. Atomic pseudo-cell contents for Huntly specimen.

The results for the Bramburg and Huntly specimens agree well with each other, but less well with Sweet's (1961) results for the Portree specimen. All three sets of results show appreciable Al₂O₃, but appreciable MgO was found only in the Portree specimen. Mitsuda (1973) has described a tobermorite specimen that was very low in MgO and associated closely with a poorly crystalline hydrous magnesium silicate mineral and concluded that tobermorite cannot accommodate appreciable MgO. This perhaps applies also to tacharanite, in which case the MgO found by Bothwell (in Sweet, 1961) must have been present in another phase.

Table II, cols. 5 and 6, gives the atomic pseudo-cell contents for the Bramburg and Huntly specimens respectively, calculated using the observed chemical analyses (cols. 2 and 3), specific gravities, and cell parameters found with X-rays. The results correspond approximately to the idealized formula Ca₁₂Al₂Si₁₈O₆₉H₃₆ if a little water is assumed to be uncombined.

Relation to tobermorite and other phases

The length of the *b*-axis (7·3 Å) in tacharanite, and its strong pseudo-halving, suggest that tacharanite contains silicon-oxygen chains kinked so as to repeat at

intervals of three tetrahedra, as in tobermorite, xonotlite, and other calcium silicate minerals. Reasoning by analogy with these minerals, the pseudo-cell may correspond to the lattice translations of the calcium–oxygen parts of the structure. In fig. 6, the pseudo-cell of tacharanite is compared with that of tobermorite (body centred orthorhombic, a 5.65, b 3.66, c 22.6 Å, McConnell, 1954). The a -axis of the pseudo-cell is approximately three times as long in tacharanite as in tobermorite, and it is possible to define similar sub-cells for the two minerals; these have a 5.69, b 3.65, c 12.7 Å, β 90.2° for tacharanite and a 5.65, b 3.66, c 11.3 Å, β 90° for tobermorite. The approximate contents of the pseudo-cell of tacharanite ($\text{Ca}_{12}\text{Al}_2\text{Si}_{18}\text{O}_{69}\text{H}_{36}$) are relatively close to those of three pseudo-cells of tobermorite ($\text{Ca}_{15}\text{Si}_{18}\text{O}_{66}\text{H}_{30}$). The two minerals thus appear to be related as regards the dimensions and contents of their pseudo-cells. In addition, there is a tendency for strong X-ray reflections

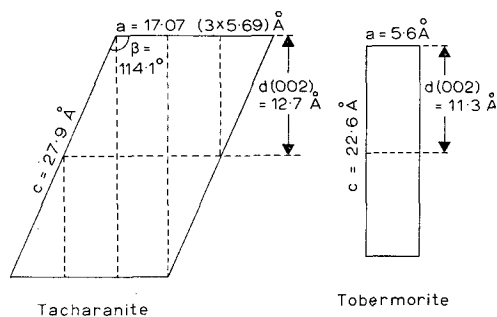


FIG. 6. Pseudo-cells of tacharanite and tobermorite, projected along the b -axis (3.65 Å) in each case. Broken lines define sub-cells, which are orthogonal for tobermorite and nearly orthogonal for tacharanite.

given by the two minerals to correspond to similar positions in reciprocal space; this explains the general similarity in powder patterns noted by Sweet (1961). The infrared spectra and t.g. curves are broadly similar. In the stability of the layer thickness to heating, tacharanite resembles so-called 'anomalous' tobermorites such as that from Loch Eynort, Scotland, studied by Gard and Taylor (1957).

While the above evidence points to a structural resemblance between the minerals, some points of difference must be emphasized. The tripling of the pseudo a -axis in tacharanite is not confined to weak reflections, and presumably indicates some important difference in structure. The fact that the pseudo-cell of tacharanite is A -centred, while that of 11.3 Å tobermorite is body-centred, means that if the tacharanite structure is based on layers similar to those in tobermorite, the lateral relation between adjacent layers differs in the two cases; in this respect, tacharanite would resemble the 9.3 Å form of tobermorite (Taylor, 1959). Tobermorite does not contain essential Al, though limited replacement of Si by Al seems to be possible; the atomic cell contents for tacharanite, in contrast, suggest that in this case Al may be an essential constituent.

The layer thickness of tacharanite (12.7 Å) differs from any of the principal values (14.0, 11.3, and 9.3 Å approx.) observed for tobermorite, and the water content, expressed as atoms of H per sub-cell, is between those found for 14.0 and 11.3 Å tobermorites. Certain tobermorites consisting principally of 14.0 Å or 11.3 Å material give weak reflections of spacing 12.3 or 12.5 Å (Heller and Taylor, 1956; Taylor, 1959), which could possibly be due to intergrown tacharanite.

Other possible similarities are to gelatinous plombierite and to the semi-crystalline

synthetic material known as C-S-H(I) or calcium silicate hydrate (I), but the X-ray and electron diffraction evidence show that tacharanite is more highly crystalline than either of these, and neither of them contains essential Al.

Acknowledgements. We thank Miss J. M. Sweet, Professor S. Koritnig, Dr. P. A. Sabine, and Dr. A. Livingstone for specimens, Dr. A. R. West for making high temperature X-ray photographs, and Dr. P. A. Sabine and Mr. B. R. Young for making available unpublished material.

REFERENCES

- CLIFF (G.) and LORIMER (G. W.), 1972. *Proc. 5th Eur. Congr. Electron Microscopy, Manchester*, 140.
 GARD (J. A.), 1971. *The Electron-Optical Investigation of Clays* (Gard, J. A., ed.) Ch. II, 45-55. Mineralogical Society, London.
 GARD (J. A.) and TAYLOR (H. F. W.), 1957. *Min. Mag.* **31**, 361.
 HELLER (L.) and TAYLOR (H. F. W.), 1956. *Crystallographic Data for the Calcium Silicates*. HMSO (London), 44.
 KORITNIG (S.), 1972. *Contr. Min. Petr.* **35**, 293.
 LIVINGSTONE (A.), 1974. *Min. Mag.* **39**, 820.
 LORIMER (G. W.) and CHAMPNESS (P. E.), 1973. *Amer. Min.* **58**, 243.
 LORIMER (G. W.), NASIR (M. J.), NICHOLSON (R. B.), NUTTALL (K.), WARD (D. E.), and WEBB (J. R.), 1972. *Proc. 5th Int. Mat. Symp.*, Berkeley, 232.
 LUCAS (J. H.), 1970. *Proc. 7th Int. Conf. Electron Microsc.* **1**, 159.
 MCCONNELL (J. D. C.), 1954. *Min. Mag.* **30**, 293.
 MIYASUDA (T.), 1973. *Cement Concr. Res.* **3**, 71.
 SABINE (P. A.) and YOUNG (B. R.), 1972. In *Ann. Rep. for 1971, Inst. Geol. Sci.* (London), 102.
 ———— 1975. *Phil. Trans. Ser. A* (in press).
 SWANSON (H. E.) and FUYAT (R. K.), 1953. *U.S. Bureau of Commerce, National Bureau of Standards Circular* 539, **2**, 20.
 SWEET (J. M.), 1961. *Min. Mag.* **32**, 745.
 TAYLOR (H. F. W.), 1959. *Proc. 6th Nat. Conf. Clays and Clay Minerals*, Berkeley 1957, 101.
 WALKER (G. P. L.), 1971. *West Commem. Vol.* [Univ. Saugar, India], 181. [M.A. 72-3476].

[Manuscript received 17 June 1974]